

## Spectroscopy of Hydrothermal Reactions 25: Kinetics of the Decarboxylation of Protein Amino Acids and the Effect of Side Chains on Hydrothermal Stability

Jun Li and Thomas B. Brill\*

Department of Chemistry and Biochemistry, University of Delaware, Newark, Delaware 19716

Received: November 25, 2002; In Final Form: April 14, 2003

The stability toward decarboxylation of six protein amino acids with functionally substituted side chains [phenylalanine (Phe), serine (Ser), threonine (Thr), proline (Pro), histidine (His), and methionine (Met)] were studied with an FT-IR spectroscopy flow reactor at  $\text{pH}_{25}$  1.5–8.5,  $T = 270\text{--}340$  °C, and  $P = 275$  bar. The first-order (or pseudo-first-order) rate constants and Arrhenius parameters were obtained on the basis of the rate of  $\text{CO}_2$  formation. The decarboxylation rates of Phe, Ser, Thr, Pro, and Met are independent of pH in the range of 3–8.5. At pH 1.5–3, a maximum rate constant occurs at about 2.5. His has a different pH–rate profile. At its natural  $\text{pH}_{25}$  (7.44), the decarboxylation rate reaches a minimum, but increasing or decreasing the pH increases the rate. The activation energies and preexponential factors for the decarboxylation of the protein amino acids cover a wide range. However, a strong correlation between  $E_a$  and  $\ln(A)$  (the kinetic compensation effect) exists, which implies that the amino acids share the same mechanism or at least the same rate-determining step regardless of the side chain. Combining the observations about decarboxylation, deamination, and dehydration, we discuss the effects of the side chains on the hydrothermal stability of protein amino acids in terms of their structures.

### Introduction

In former papers,<sup>1,2</sup> the kinetics of decarboxylation of aliphatic amino acids [glycine (Gly), alanine (Ala),  $\alpha$ -aminobutyric acid ( $\alpha$ -Aib), valine (Val), leucine (Leu), isoleucine (Ile), and  $\beta$ -aminobutyric acid ( $\beta$ -Aib)] were studied at different solution pH values. It was found that (1) the decarboxylation of these amino acids followed first-order or pseudo-first-order kinetics; (2) the relative decarboxylation rates of these amino acids were in order  $\text{Gly} > \text{Leu} \approx \text{Ile} \approx \text{Val} > \text{Ala} > \alpha\text{-Aib} > \beta\text{-Aib}$ ; (3) increasing the ionic strength retarded decarboxylation, leading to the inference that the transition-state structures were less polar than the reactants; (4) the pH–rate profiles of decarboxylation have an inverse trend compared to the trend for racemization; and (5) the hydrothermal stability of aliphatic amino acids increased as the amino group was moved farther from the carboxylate group (i.e.,  $\gamma > \beta > \alpha$ ).

This paper focuses on the effects that functionally substituted side chains containing hydroxyl (Ser and Thr), aryl (Phe), pyrrolidine (Pro), imidazole (His), and thioether (Met) have on the kinetics of decarboxylation. The remaining protein amino acids that are not studied are either too insoluble in water to be monitored by the FT-IR flow reactor or deaminate and release ammonia, which is not detected owing to interference by the water absorption bands. Combining the present observations with those from the literature<sup>1–18</sup> about the decarboxylation, deamination, and dehydration of protein amino acids enables the effects of side chains on the hydrothermal stability to be discussed. An understanding of the hydrothermal stability of protein amino acids is needed to assess their role in extreme environments.

### Experimental Section

Protein amino acids Ser, Thr, Phe, Pro, His, and Met were purchased from Sigma-Aldrich Co. and used without further purification. They were dissolved in milli-Q deionized water at concentrations controlled to be 0.05 to 0.1 *m*. The pH was adjusted as desired in the 1.5–8.5 range by titrating with aqueous HCl or NaOH solution and recorded on an Orion model 330 pH meter.

The flow reactor FT-IR spectroscopy cell constructed from titanium with sapphire windows and gold foil seals has been described in detail elsewhere.<sup>19,20</sup> The experimental procedure used here is the same as that reported in former papers.<sup>1,2</sup> In addition to the in situ spectral measurements, batch-mode experiments were first conducted to determine whether solid decomposition products formed, which could plug the flow reactor. No problems were encountered provided the reaction time was kept relatively short. Because of corrosion and leaking, the flow reactor was used below 340 °C, although one experiment was performed on Pro at 340 °C at its natural pH. Kinetic experiments above pH 8.5 were not conducted because of the low solubility of the amino acid and the hydrolysis of  $\text{CO}_2$ .<sup>21</sup> The asymmetric stretch of aqueous  $\text{CO}_2$  centered at 2343  $\text{cm}^{-1}$  was observed with in situ FT-IR spectroscopy in the band pass of sapphire and the pH range of 1.5–8.5. The band area of  $\text{CO}_2$  was converted into concentration at each condition by using the Beer–Lambert law and the previously determined molar absorptivity of aqueous  $\text{CO}_2$ .<sup>22</sup> A detailed discussion of the hydrolysis of  $\text{CO}_2$  and the validity of replacing the total  $\text{CO}_2$  concentration by the observed  $\text{CO}_2$  concentration in the pH range of 1.5–8.5 is available.<sup>1</sup> Briefly, the in situ FT-IR spectroscopy flow reactor kinetics experiments require that the observed  $\text{CO}_2$  concentration be corrected by knowing the pH at high temperatures. The true pH values at high temperatures can be calculated from a charge-balance equation given the

\* Corresponding author. E-mail: brill@udel.edu.

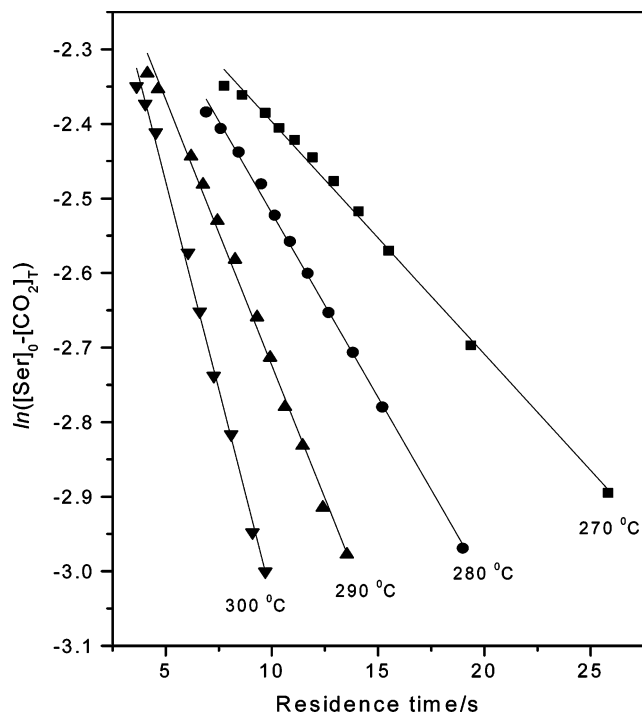


**Figure 1.** First-order rate plot for the decarboxylation of 0.1 *M* Ser at its natural pH and 275 bar.

ionization constants for all of the contributing species. The required ionization constants of CO<sub>2</sub> species, the reactants, and the products at high temperatures could be extrapolated from room temperature via the iso-Coulombic method<sup>23</sup> using the ionization constant<sup>24</sup> and specific volume<sup>25</sup> of water. In the pH range of 1.5–7, water at high-temperature shifts the solution pH toward neutral, and the hydrolysis of CO<sub>2</sub> is less compared to that at room temperature. During the decarboxylation of amino acids, the reactants and products also buffer the solution. Weighted least-squares regression<sup>26</sup> with a 95% confidence interval was performed in which the statistical weight was set to  $1/\sigma^2$ , where  $\sigma$  is the standard deviation of the variables.

## Results and Discussion

**Kinetics.** On the basis of the rate of CO<sub>2</sub> formation, the observed decarboxylation rate constants varied with pH and were obtained by plotting  $\ln([\text{amino acid}]_0 - [\text{CO}_2]_T)$  versus residence time, where  $[\text{amino acid}]_0$  is the initial concentration of amino acid and  $[\text{CO}_2]_T$  is the total CO<sub>2</sub> concentration, which can be replaced by the observed CO<sub>2</sub> concentration in the pH range of 1.5–8.5 without loss of accuracy in the calculation of the rate constants. Most decarboxylation reactions followed the first-order or pseudo-first-order rate law at least to 40% conversion (Figure 1), but the decomposition process of Met was better represented by two rate constants. That is, a first-order rate constant fit the data at lower temperatures during an obvious induction period. As the decarboxylation process continued, it appeared to have autocatalytic behavior that fit a second-order rate constant. The thioetheramine product appeared to be the logical catalyst for the reaction because the coproduct CO<sub>2</sub> did not affect the rate in any of the other amino acids. The presence of a thiol group also accelerated the deamination reaction.<sup>16</sup> The observed rate constants varied with pH and are listed in Table 1. The pH versus rate profiles of the observed rate constants at 300 °C are displayed in Figure 2. In the case of Pro, the temperature is 320 °C. The same trend in the rate constants as

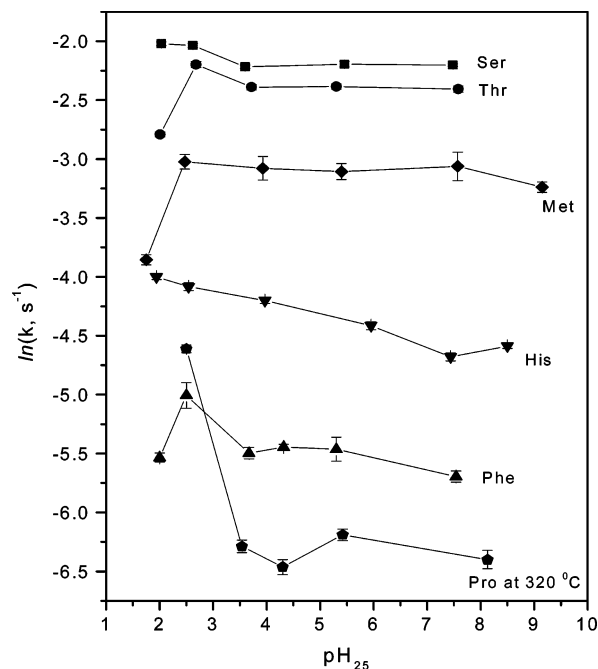


**Figure 2.** pH–rate profile of Ser, Thr, Met, His, and Phe at 300 °C and Pro at 320 °C and 275 bar.

a function of pH was observed for aliphatic amino acids.<sup>1</sup> Except for His, the observed rate constants are essentially independent of pH in the range of 3–8.5. This is the buffered zwitterion region. When the pH is below 3, the rate constant is maximized at about 2.5 and then decreases again at lower pH. At its natural pH<sub>25</sub> (7.44), His exhibited the minimum decarboxylation rate in the zwitterion form, and increasing or decreasing the pH increased the rate. This phenomenon for His might be explained by the tautomerization equilibrium of the zwitterion and anion forms of the imidazole ring (Scheme 1)<sup>27–30</sup> in neutral and basic solutions. The pairs of tautomers have different rate constants. The observed rate constant reflects the contribution of all reactive species at a given pH and temperature. Protonation of the imidazole ring caused the decarboxylation rate to increase with decreasing solution pH.

The variation of the decarboxylation rate with temperature followed the Arrhenius rate law. Figure 3 shows the Arrhenius plots of Ser, Thr, Phe, His, Met, and Pro, including the present data and that of other authors. It should be noted that the decomposition rate constants for Ser and Thr by Vallentyne<sup>12</sup> and Anderson and Holm<sup>4</sup> are combinations of dehydration and decarboxylation. At hydrothermal conditions, Ser and Thr decompose via three competitive pathways: dehydration, decarboxylation, and aldol cleavage.<sup>18</sup> The dehydration pathway accounts for about 10% of the total decomposition. This result was confirmed by the fact that the ratio of the largest CO<sub>2</sub> concentration to the initial Thr concentration was about 0.88. Consequently, the aldol cleavage decomposition pathway for Ser and Thr is not significant. When this conclusion holds, the combined first-order decomposition rate constants for dehydration and decarboxylation are obtained by multiplying the decarboxylation rate constants by 1.14 because dehydration also followed first-order kinetics. From the comparisons in Figure 3 and former data<sup>1</sup> for the aliphatic amino acids, it can be seen that the decarboxylation rate constants determined by using the batch and postreaction analysis methods are underestimated compared to those determined by in situ FT-IR spectroscopy using the titanium flow reactor. The reason is unclear at this time.

**TABLE 1: Observed Pseudo-First-Order Rate Constants ( $k_{\text{obs}} \times 10^3 \text{ s}^{-1}$ ) for the Decarboxylation of  $\alpha$ -Amino Acids at 275 bar and Different Solution pH Values<sup>a</sup>**

Serine (0.1 m), pH <sub>25</sub>						
temp (°C)	2.03	2.62	3.60	5.45 (nat) <sup>b</sup>	7.48	
270	43.64 ± 0.93	35.93 ± 0.59	28.61 ± 0.96	29.91 ± 0.91	29.15 ± 0.58	
280	66.00 ± 1.12	54.51 ± 0.85	42.29 ± 1.15	48.45 ± 0.97	44.47 ± 1.32	
290	94.86 ± 1.38	82.69 ± 1.55	67.90 ± 2.17	69.73 ± 1.65	69.36 ± 2.09	
300	132.38 ± 2.08	130.52 ± 2.27	108.97 ± 1.46	111.40 ± 2.50	110.53 ± 1.43	
Threonine (0.1 m), pH <sub>25</sub>						
temp (°C)	2.01	2.68	3.72	5.30 (nat) <sup>b</sup>	7.58	
270	17.81 ± 0.76	19.90 ± 0.24	19.67 ± 0.41	17.55 ± 0.35	17.38 ± 0.40	
280	28.46 ± 0.68	36.76 ± 0.83	34.51 ± 0.61	32.70 ± 0.71	32.42 ± 0.86	
290	42.76 ± 0.75	62.02 ± 1.25	53.56 ± 1.76	53.94 ± 1.28	51.84 ± 1.58	
300	61.36 ± 1.30	111.05 ± 2.83	91.67 ± 2.13	92.16 ± 2.05	90.17 ± 2.41	
Phenylalanine (0.05 m), pH <sub>25</sub>						
temp (°C)	2.00	2.50	3.67	4.32	5.30 (nat) <sup>b</sup>	7.54
300	3.95 ± 0.15	6.70 ± 0.73	4.10 ± 0.20	4.32 ± 0.10	4.24 ± 0.43	3.36 ± 0.16
310	8.23 ± 0.23	15.56 ± 0.95	8.86 ± 0.33	7.87 ± 0.23	9.07 ± 0.23	8.62 ± 0.21
320	17.89 ± 0.67	30.44 ± 1.08	17.11 ± 0.66	16.99 ± 0.39	17.62 ± 0.78	14.68 ± 0.26
330	28.32 ± 1.02	51.88 ± 2.05	29.85 ± 1.28	28.48 ± 0.39	28.64 ± 0.73	24.74 ± 0.48
Proline (0.1 m), pH <sub>25</sub>						
temp (°C)	2.04	2.50	3.54	4.30	5.42 (nat) <sup>b</sup>	8.13
320		9.93 ± 0.32	1.86 ± 0.10	1.56 ± 0.10	2.05 ± 0.10	1.66 ± 0.13
330		20.19 ± 0.78	3.52 ± 0.15	3.44 ± 0.18	3.94 ± 0.15	3.53 ± 0.24
340					7.17 ± 0.37	
Histidine (0.05 m), pH <sub>25</sub>						
temp (°C)	1.94	2.54	3.97	5.95	7.44 (nat) <sup>b</sup>	8.5
300	18.30 ± 0.40	16.84 ± 0.54	14.97 ± 0.37	12.10 ± 0.39	9.28 ± 0.31	10.17 ± 0.18
310	36.08 ± 1.61	28.50 ± 0.78	27.08 ± 0.76	22.40 ± 0.60	16.93 ± 0.58	15.75 ± 0.49
320	65.01 ± 1.32	54.47 ± 1.38	45.58 ± 0.85	35.43 ± 0.95	30.33 ± 0.97	26.19 ± 0.69
330	113.71 ± 4.87	82.57 ± 1.81	75.90 ± 2.70	54.67 ± 1.76	45.31 ± 1.16	41.56 ± 1.89
Methionine (0.1 m), pH <sub>25</sub>						
temp (°C)	1.75	2.47	3.93	5.40 (nat) <sup>b</sup>	7.57	9.15
270		6.64 ± 0.17	11.21 ± 0.56	10.50 ± 0.59	8.82 ± 0.95	
280	5.13 ± 0.15	14.96 ± 0.40	20.54 ± 1.59	17.93 ± 1.90	17.01 ± 1.22	12.87 ± 0.41
290	13.19 ± 0.48	28.19 ± 1.34	33.17 ± 1.45	28.39 ± 2.32	26.57 ± 1.62	25.30 ± 0.74
300	21.17 ± 0.91	48.65 ± 3.03	46.04 ± 4.61	44.73 ± 3.05	46.80 ± 5.66	39.22 ± 1.75

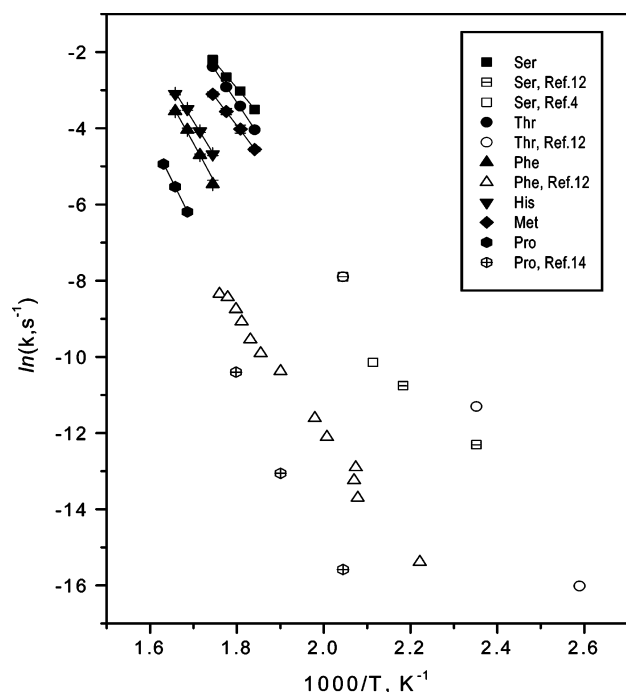
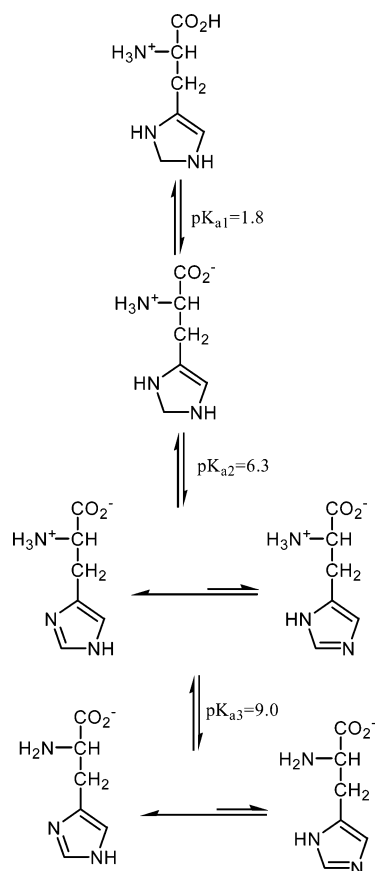
<sup>a</sup> pH is given at room temperature. <sup>b</sup> Natural pH.

Table 2 gives the Arrhenius parameters for the decarboxylation of protein amino acids and the deamination of aspartic acid (Asp).<sup>17</sup> The values lie in the range of 108–135 kJ/mol for racemization.<sup>31,32</sup> Figure 4 shows that a strong kinetic compensation effect<sup>33–35</sup> exists when a plot of  $E_a$  versus  $\ln(A)$  for decarboxylation is made. The existence of a kinetic compensation effect suggests that the protein amino acids share a common decarboxylation mechanism or at least the same rate-determining step regardless of the side chain. The mechanism of decarboxylation is the subject of the following paper.<sup>36</sup>

**Effect of the Side Chain on Hydrothermal Stability.** The side chains of protein amino acids consist of alkyl, aryl, indole, pyrrolidine, imidazole, carboxylic acid, amine, guanidino, hydroxyl, amide, and thioether groups. In neutral aqueous solution, these side chains can be divided into three categories: apolar groups, uncharged polar groups, and charged groups. It is not surprising that the decomposition of protein amino acids is complicated by differences in the functional groups. Not counting changes in the optical activity, three destructive pathways—decarboxylation, deamination (at the  $\alpha$  position and side chains), and dehydration—occur for protein amino acids. Although both decarboxylation and deamination (at the  $\alpha$  position) follow first-order kinetics, the mechanisms are probably different. Deamination takes place through a carbanion mechanism.<sup>17</sup> In the following paper,<sup>36</sup> the mechanism of the

decarboxylation of amino acids in which the formation of a water molecule-assisted transition-state structure is rate-determining is analyzed. Decarboxylation usually occurs at higher temperatures than does deamination. Among 20 protein amino acids, 5 amino acids [asparagine (Asn), Asp, Cys, glutamine (Gln), and arginine (Arg)] are known to deaminate faster than they decarboxylate<sup>16</sup> in the order Asn > Gln > Cys > Asp > Arg. Asp undergoes reversible deamination at the  $\alpha$  position if ammonia is present in solution (Scheme 2).<sup>17</sup> This process is better understood as resulting from an intramolecular interaction following the explanation of faster racemization of Asp over Ala.<sup>31,32</sup> Asn deaminates at both the amide terminus of the side chain and at the  $\alpha$  position.<sup>16</sup> There is reason to believe that the amide terminus hydrolyzes first to Asp and then Asp deaminates (Scheme 3).<sup>37</sup> Gln, however, can undergo either hydrolysis first to glutamic acid (Glu) with the release of  $\text{NH}_3$ , followed by the cyclization of Glu to form pyroglutamic acid, or cyclization directly to pyroglutamic acid with the release of  $\text{NH}_3$ , as shown in Scheme 4. It is known that Glu dehydrates via cyclization to produce pyroglutamic acid (Scheme 5).<sup>13</sup> The resultant pyroglutamic acid has high thermal stability and decomposes through hydrolysis to Glu, which then decarboxylates directly. In fact, the fast equilibrium between Glu and pyroglutamic acid lies more toward pyroglutamic acid.  $\alpha$ -Amino adipic acid cyclizes more easily to form six-membered piperi-

## SCHEME 1



**Figure 3.** Arrhenius plot and comparison with previously reported results for Ser, Thr, Met, His, and Phe at 275 bar. The solid symbols are from the present work.

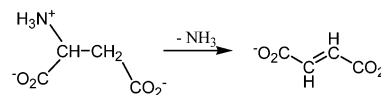
dine than does Glu to form five-membered pyrrolidine.<sup>31</sup> In the gas phase, Arg may exist in the neutral or zwitterionic form depending on the presence of a water molecule or metal cations.<sup>38,39</sup> Decomposition occurs by dehydration or deamination.<sup>38</sup> In addition, the hydrolysis<sup>40</sup> of the guanidino terminus

**TABLE 2: Arrhenius Parameters of Amino Acid Decomposition and Relative Decarboxylation Rates at 320 °C**

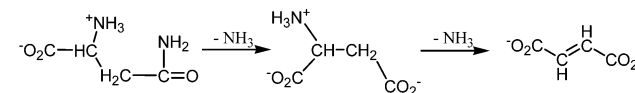
amino acid	$E_a$ (kJ·mol <sup>-1</sup> )	ln(A) (s <sup>-1</sup> )	rel rate at 320 °C
alanine	190.55 ± 7.36	34.01 ± 1.49	1
glycine	175.50 ± 8.25 <sup>a</sup>	30.09 ± 1.99 <sup>a</sup>	6.06
	165.70 <sup>b</sup>	28.40 <sup>b</sup>	
α-aminobutyric acid	207.22 ± 7.40	36.81 ± 1.49	0.56
valine	185.89 ± 4.01	33.58 ± 0.81	1.57
leucine	141.99 ± 4.41	24.84 ± 0.89	1.91
	189.12 <sup>c</sup>	32.77 <sup>c</sup>	
isoleucine	180.77 ± 12.31	32.51 ± 2.47	1.65
serine	110.93 ± 4.65	21.07 ± 1.00	23.72
	122.80 <sup>d</sup>	28.32 <sup>d</sup>	
threonine	142.11 ± 3.41	27.44 ± 0.74	24.79
	141.25 <sup>d</sup>	28.22 <sup>d</sup>	
phenylalanine	171.03 ± 7.88	30.57 ± 1.6	1.73
	128.87 <sup>d</sup>	18.95 <sup>d</sup>	
histidine	151.76 ± 7.97	27.20 ± 1.62	2.98
methionine	125.04 ± 1.61	23.15 ± 0.35	10.69
proline	189.40 ± 3.52	32.22 ± 0.70	0.20
	177.40 <sup>e</sup>	28.04 <sup>e</sup>	
pyroglutamic acid	149.79 <sup>e</sup>	21.42 <sup>e</sup>	
aspartic acid	Deamination		
	153.97 <sup>f</sup>	33.04 <sup>f</sup>	

<sup>a</sup> Regressed on the basis of the overall reported data, except for that in ref 8. <sup>b</sup> Snider, M. J. College of Wooster. Personal communication, 2002. <sup>c</sup> Reference 14. <sup>d</sup> Reference 12. <sup>e</sup> Reference 13. <sup>f</sup> Reference 17.

## SCHEME 2



## SCHEME 3



of Arg releases NH<sub>3</sub> to liberate the nonprotein amino acid ornithine (HCO<sub>2</sub>CH(NH<sub>2</sub>)(CH<sub>2</sub>)<sub>3</sub>NH<sub>2</sub>) and then intramolecularly dehydrates, forming 3-aminopiperidine-2-one (Scheme 6). The hydrothermolysis of guanidine has been explored.<sup>20,41</sup> The expected reaction is slow hydrolysis at hydrothermal conditions when the amino group is located at the chain terminus. In general, intramolecular cyclization to produce a lactam is explained by the “gauch effect”<sup>42</sup> when the conditions of a suitable carbon chain length and the presence of electronegative groups at the two chain termini are met. The gauch effect originates from hyperconjugation.<sup>43</sup> The ease of intramolecular cyclization by dehydration and deamination for amino acids is related to the strain in the resulting ring.<sup>44</sup>

It has been observed that spontaneous decarboxylation takes place for protein amino acids when the side chains contain alkyl, aryl, hydroxyl, pyrrolidine, imidazole, and thioether groups. Their relative decarboxylation rates are indicated in Table 2. Both electronic and steric effects of the side chains influence the decarboxylation rate, but it seems that the electronic effect is more significant. When a hydrogen atom in the amino group is replaced by a halo atom, the resulting *N*-halo-α-amino acids are unstable at room temperature in aqueous solution and decompose via concerted fragmentation to produce CO<sub>2</sub>, halo ion, NH<sub>3</sub>, and the imine. The imine then rapidly hydrolyzes to the ketone or aldehyde.<sup>45–52</sup> Experimental studies<sup>45–50</sup> showed that decomposition followed first-order kinetics and was independent of pH in the range of 3–12. Beyond this pH range, increasing<sup>48</sup> and decreasing<sup>50</sup> the pH increased the rate, which

## SCHEME 4

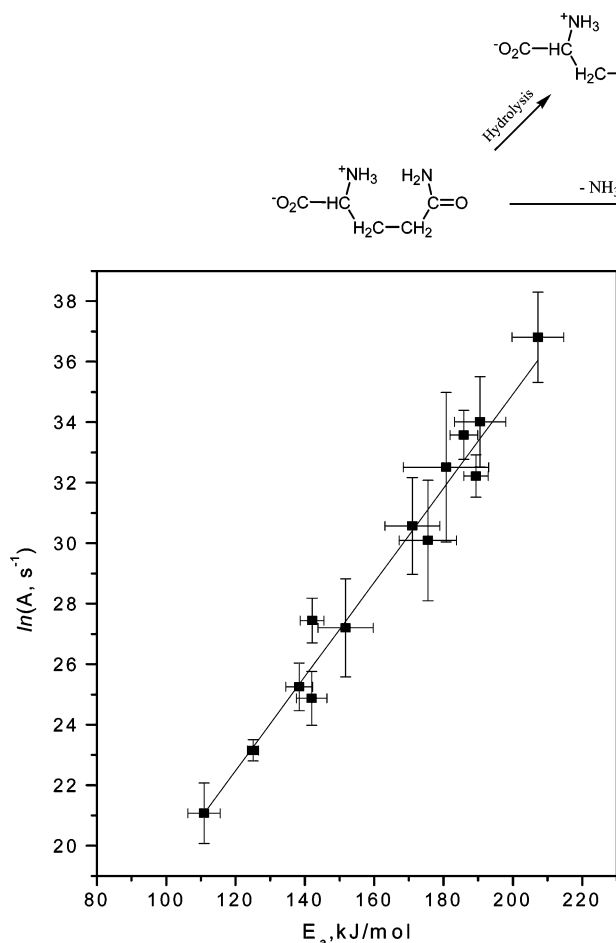
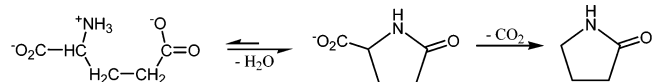


**Figure 4.** Kinetic compensation effect for the decarboxylation of  $\alpha$ -amino acids (Table 2).

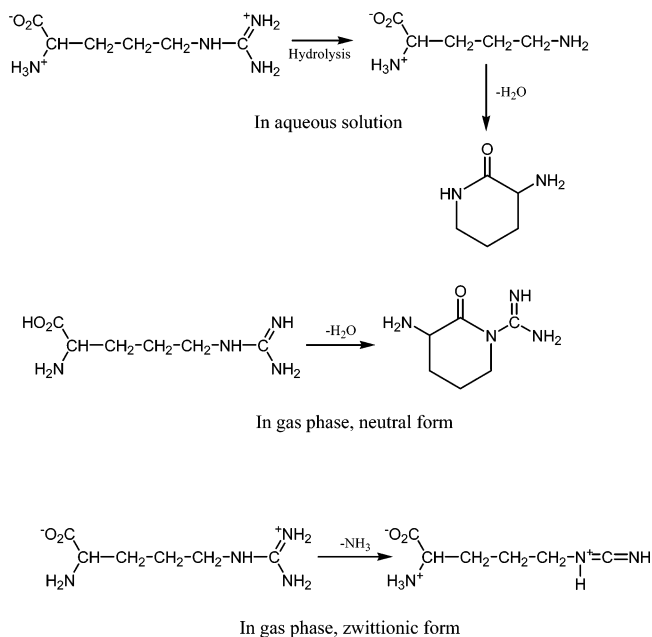
## SCHEME 5



suggests that acid and base catalysis occur. The alkyl substituents at both the N atom of the amino group and the  $\alpha$  carbon increased the rate constants. Moreover, increasing the bulk and number of alkyl substituents reduced the barrier height and enhanced the rate of decomposition. The effect of the side chains on the decomposition rate of *N*-halo- $\alpha$ -amino acids is the same for  $\alpha$ -amino acids, although the trend in the rate variation differed. Rates increased for *N*-halo- $\alpha$ -amino acids when the linear carbon chain increased in length (i.e., Gly < Ala < Aib) or the carbon chain further lengthened and then branched, but this latter effect was smaller than the effect that occurred with shorter linear carbon chains. For  $\alpha$ -amino acids, the decarboxylation rate decreased when the linear carbon chain lengthened (i.e., Gly > Ala > Aib). Increasing carbon chain length in a branched mode increased the rate, but the effect was small. Therefore, the effect of aliphatic carbon chains on the reaction rate is complicated by both electronic and steric effects. The electronic effect is further complicated by the balance of inductive and hyperconjugative differences. Because the mechanisms for the decomposition of *N*-halo- $\alpha$ -amino acids and the decarboxylation of  $\alpha$ -amino acids are different, the influence of the aliphatic side chain is different.

An interesting phenomenon was found for the decomposition of amino acids with a sulfur heteroatom in the side chain (Cys

## SCHEME 6



and Met). The deamination of Cys occurs more easily than decarboxylation, whereas Met decarboxylates more easily compared to deamination. These two amino acids share a similar kinetic process; that is, the deamination of Cys and the decarboxylation of Met both fit an autocatalytic model. The decomposition products containing the thiol group might act as a catalyst to promote decarboxylation and deamination. Kovacs et al.<sup>53</sup> suggested that orbital overlap enhanced the stability of the enolate, resulting in an increased rate of racemization over Ala, but Smith et al.<sup>32</sup> believed that a dispersed negative charge on the carboxylate group increased the racemization rate. A more complete interpretation should come from an electronic structure calculation.

In summary, the side chains of aqueous amino acids can alter the decarboxylation rates by a factor of up to about 120 at 320°C. The strong kinetic compensation effect in the Arrhenius parameters makes it risky to extrapolate the rates outside the temperature range of measurement. In the following paper, a mechanism by which amino acids decarboxylate is proposed.

**Acknowledgment.** We are grateful to the National Science Foundation for supporting of this work through grant CHE-9807370.

## References and Notes

- (1) Li, J.; Brill, T. B. To be submitted for publication.
- (2) Li, J.; Wang, X. G.; Klein, M. T.; Brill, T. B. *Int. J. Chem. Kinet.* **2002**, *34*, 271.
- (3) Kohara, M.; Gamo, T.; Yanagawa, H.; Kobayashi, K. *Chem. Lett.* **1997**, 1053.
- (4) Anderson, E.; Holm, N. G. *Origins Life Evol. Biosphere* **2000**, *30*, 9.

- (5) Miller, S. L.; Bada, J. L. *Nature* **1988**, *334*, 609.
- (6) Bada, J. L.; Miller, S. L.; Zhao, M. *Origins Life Evol. Biosphere* **1995**, *25*, 111.
- (7) Bada, J. L. *Philos. Trans. R. Soc. London, Ser. B* **1991**, *333*, 349.
- (8) Qian, Y.; Engel, M. H.; Macko, S. A.; Carpenter, S. C.; Deming, J. W. *Geochim. Cosmochim. Acta* **1993**, *57*, 3281.
- (9) Abelson, P. H. *Geol. Soc. Am.* **1957**, *67*, 87.
- (10) Conway, D.; Libby, W. F. *J. Am. Chem. Soc.* **1958**, *80*, 1077.
- (11) Snider, M. J.; Wolfenden, R. *J. Am. Chem. Soc.* **2000**, *122*, 11507.
- (12) Vallentyne, J. R. *Geochim. Cosmochim. Acta* **1964**, *28*, 157.
- (13) Povoledo, D.; Vallentyne, J. R. *Geochim. Cosmochim. Acta* **1964**, *28*, 731.
- (14) Vallentyne, J. R. *Geochim. Cosmochim. Acta* **1968**, *32*, 1353.
- (15) Quitain A. T.; Sato, N.; Lee, J.-O.; Daimon, H. *5th International Conference on Solvo-Thermal Reactions*, July, 2002, East Brunswick, N. J., p 98.
- (16) Sohn, M.; Ho, C.-T. *J. Agric. Food Chem.* **1995**, *43*, 3001.
- (17) Bada, J. L.; Miller, S. L. *J. Am. Chem. Soc.* **1970**, *92*, 2774.
- (18) Bada, J. L.; Shou, M. Y.; Man, E. H.; Schroeder, R. A. *Earth Planet. Sci. Lett.* **1978**, *41*, 67.
- (19) Kieke, M. L.; Schoppelrei, J. W.; Brill, T. B. *J. Phys. Chem.* **1996**, *100*, 7455.
- (20) Schoppelrei, J. W.; Kieke, M. L.; Wang, X.; Klein, M. T.; Brill, T. B. *J. Phys. Chem.* **1996**, *100*, 14343.
- (21) Butler, J. N. *Ion Equilibrium, Solubility and pH Calculation*; Wiley & Sons: New York, 1998; p 368.
- (22) Maiella, P. G.; Schoppelrei, J. W.; Brill, T. B. *Appl. Spectrosc.* **1999**, *53*, 351.
- (23) Lindsay, W. T. *Proc. Int. Water Conf. Eng. Soc. W. Pa.* **1980**, *41*, 284.
- (24) Uematsu, M.; Franck, E. U. *J. Phys. Chem. Ref. Data* **1980**, *9*, 1291.
- (25) Marshall, W. L.; Franck, E. U. *J. Phys. Chem. Ref. Data* **1981**, *10*, 295.
- (26) Cvetanovic, R. J.; Singleton, D. L. *Int. J. Chem. Kinet.* **1977**, *9*, 481.
- (27) Farr-Jones, S.; F. J.; Wong, W. Y. L.; Gutheil, W. G.; Bachovchin, W. W. *J. Am. Chem. Soc.* **1993**, *115*, 6813.
- (28) Bachovchin, W. W.; Herzfeld, W. W.; Dobson, C. M.; Griffin, R. G. *J. Am. Chem. Soc.* **1982**, *104*, 1192.
- (29) Blomberg, F.; Maurer, W.; Ruterjans, H. *J. Am. Chem. Soc.* **1977**, *99*, 8149.
- (30) Alei, M.; Morgan, L. O.; Wageman, W. E.; Waley, T. W. *J. Am. Chem. Soc.* **1980**, *102*, 2881.
- (31) Liardon, R.; Ledermann, S. *J. Agric. Food Chem.* **1986**, *34*, 557.
- (32) Smith, G. G.; Reddy, G. V. *J. Org. Chem.* **1989**, *54*, 4529.
- (33) Liu, L.; Guo, Q. X. *Chem. Rev.* **2001**, *101*, 673.
- (34) Bell, J. L. S.; Palmer, D. A. In *Organic Acids in Geological Processes*; Pittman, E. D., Lewan, M. D., Eds.; Springer-Verlag: Berlin, 1994; p 226.
- (35) Brill, T. B.; Gongwer, P. E.; Williams, G. K. *J. Phys. Chem.* **1994**, *98*, 12242.
- (36) Li, J.; Brill, T. B. *J. Phys. Chem. A*, **2003**, *107*, 5993.
- (37) Belsky, A. J.; Maiella, P. G.; Brill, T. B. *J. Phys. Chem. A* **1999**, *103*, 4253.
- (38) Murray, K.; Rasmussen, S.; Neutraedter, J. Luch, J. M. *J. Biol. Chem.* **1965**, *240*, 705.
- (39) Jockusch, R. A.; Price, W. D.; Williams, E. R. *J. Phys. Chem. A* **1999**, *103*, 9266.
- (40) Price, W. D.; Jockusch, R. A.; Williams, E. R. *J. Am. Chem. Soc.* **1997**, *119*, 11988.
- (41) Price, D. J.; Roberts, J. D.; Jorgensen, W. L. *J. Am. Chem. Soc.* **1998**, *120*, 9672.
- (42) Pophristic, V.; Goodman, L. *Nature* **2001**, *411*, 565.
- (43) Belsky, A. J.; Brill, T. B. *J. Phys. Chem. A* **1999**, *103*, 7826.
- (44) March, L. *Advanced Organic Chemistry*, 4th ed.; Wiley & Sons: New York, 1992.
- (45) Stambro, W. D.; Smith, W. D. *Environ. Sci. Technol.* **1979**, *13*, 446.
- (46) Hand, V. C.; Snyder, M. P.; Margerum, D. W. *J. Am. Chem. Soc.* **1983**, *105*, 4022.
- (47) Awad, R.; Hussain, A.; Crooks, P. A. *J. Chem. Soc., Perkin Trans. 2* **1990**, 1233.
- (48) Abia, L.; Armesto, X. L.; Canle, L. M.; Garcia, M. V.; Losada, M.; Santaballa, J. A. *Int. J. Chem. Kinet.* **1994**, *26*, 1041.
- (49) Armesto, X. L.; Canle, L. M.; Losada, M.; Santaballa, J. A. *J. Org. Chem.* **1994**, *59*, 4659.
- (50) Antelo, J. M.; Arce, F.; Fanco, J.; Rodriguez, P.; Varela, A. *Int. J. Chem. Kinet.* **1988**, *20*, 433.
- (51) Queralt, J. J.; Safont, V. S.; Moliner, V.; Andres, J. *Chem. Phys.* **1998**, *229*, 125.
- (52) Andres, J.; Queralt, J. J.; Safont, V. S.; Canle, M.; Santaballa, J. A. *J. Phys. Chem.* **1996**, *100*, 3561.
- (53) Kovacs, J.; Holleran, E. M.; Hui, K. Y. *J. Org. Chem.* **1980**, *45*, 1060.